



# Differential regulation of PD-L1 expression by immune and tumor cells in NSCLC and the response to treatment with atezolizumab (anti-PD-L1)

Marcin Kowanetz<sup>a,1</sup>, Wei Zou<sup>a</sup>, Scott N. Gettinger<sup>b</sup>, Hartmut Koeppen<sup>a</sup>, Mark Kockx<sup>c</sup>, Peter Schmid<sup>d</sup>, Edward E. Kadel III<sup>a</sup>, Ignacio Wistuba<sup>e</sup>, Jamie Chaff<sup>f</sup>, Naiyer A. Rizvi<sup>g</sup>, David R. Spigel<sup>h</sup>, Alexander Spira<sup>i</sup>, Fred R. Hirsch<sup>j</sup>, Victor Cohen<sup>k</sup>, Dustin Smith<sup>a</sup>, Zach Boyd<sup>a</sup>, Natasha Miley<sup>a</sup>, Susan Flynn<sup>a</sup>, Vincent Leveque<sup>a</sup>, David S. Shames<sup>a</sup>, Marcus Ballinger<sup>a</sup>, Simonetta Mocci<sup>a</sup>, Geetha Shankar<sup>a</sup>, Roel Funke<sup>a</sup>, Garret Hampton<sup>a</sup>, Alan Sandler<sup>a</sup>, Lukas Amler<sup>a</sup>, Ira Mellman<sup>a,1</sup>, Daniel S. Chen<sup>a</sup>, and Priti S. Hegde<sup>a</sup>

<sup>a</sup>Oncology Biomarker Development, Genentech, Inc., South San Francisco, CA 94080; <sup>b</sup>Medical Oncology, Yale Cancer Center, New Haven, CT 06510; <sup>c</sup>HistoGeneX, 2610 Antwerp, Belgium; <sup>d</sup>Barts Cancer Institute, Queen Mary University of London, London EC1M 6BQ, United Kingdom; <sup>e</sup>Translational Molecular Pathology, MD Anderson Cancer Center, Houston, TX 77054; <sup>f</sup>Medical Oncology, Memorial Sloan Kettering Cancer Center, New York, NY 10065; <sup>g</sup>Hematology and Oncology, Columbia University, New York, NY 10027; <sup>h</sup>Sarah Cannon Research Institute, Nashville, TN 37203; <sup>i</sup>Oncology Program, Virginia Cancer Specialists, Fairfax, VA 22031; <sup>j</sup>Medical Oncology, University of Colorado Cancer Center, Denver, CO 80045; and <sup>k</sup>Oncology, Jewish General Hospital, Montreal, QC, Canada H3T 1E2

Edited by Dennis A. Carson, University of California, San Diego, La Jolla, CA, and approved August 21, 2018 (received for review August 21, 2018)

**Programmed death-ligand 1 (PD-L1) expression on tumor cells (TCs) by immunohistochemistry is rapidly gaining importance as a diagnostic for the selection or stratification of patients with non-small cell lung cancer (NSCLC) most likely to respond to single-agent checkpoint inhibitors. However, at least two distinct patterns of PD-L1 expression have been observed with potential biological and clinical relevance in NSCLC: expression on TC or on tumor-infiltrating immune cells (ICs). We investigated the molecular and cellular characteristics associated with PD-L1 expression in these distinct cell compartments in 4,549 cases of NSCLC. PD-L1 expression on IC was more prevalent and likely reflected IFN- $\gamma$ -induced adaptive regulation accompanied by increased tumor-infiltrating lymphocytes and effector T cells. High PD-L1 expression on TC, however, reflected an epigenetic dysregulation of the PD-L1 gene and was associated with a distinct histology described by poor immune infiltration, sclerotic/desmoplastic stroma, and mesenchymal molecular features. Importantly, durable clinical responses to atezolizumab (anti-PD-L1) were observed in patients with tumors expressing high PD-L1 levels on either TC alone [40% objective response rate (ORR)] or IC alone (22% ORR). Thus, PD-L1 expression on TC or IC can independently attenuate anticancer immunity and emphasizes the functional importance of IC in regulating the antitumor T cell response.**

PD-L1 | cancer immunotherapy | atezolizumab | checkpoints | PD-1

Agents that target the programmed death-ligand 1 (PD-L1)/programmed death-1 (PD-1) axis now constitute standard of care in patients with metastatic non-small cell lung cancer (NSCLC) who are either chemotherapy naive or were previously treated with platinum-based doublet chemotherapy (1–7). In the frontline setting, pembrolizumab (anti-PD-1 antibody) has been approved as a monotherapy in patients with tumors that are highly positive for PD-L1 on tumor cells (TCs; tumor proportion score of  $\geq 50\%$ ) (5), thus making PD-L1 testing a mandatory diagnostic test for treatment planning. In the second-line (2L) setting and beyond, atezolizumab (anti-PD-L1 antibody) has been approved as monotherapy in PD-L1-unselected NSCLC patients based on overall survival (OS) benefit observed across all PD-L1 expression subgroups in a phase 3 clinical trial OAK, comparing efficacy of atezolizumab versus docetaxel in patients with previously treated NSCLC (1, 6). However, even here, patients with high PD-L1 expression on TCs or tumor-infiltrating immune cells (ICs) exhibited the strongest survival benefit. Although these observations suggest that PD-L1 expression on TC and IC plays nonredundant roles in regulating the antitumor T

cell response, the mechanistic significance of PD-L1 on TC vs. IC is unclear.

PD-L1 expression is generally thought to be induced at the transcriptional level after exposure to IFN- $\gamma$  released by T effector cells ( $T_{eff}$ s) (8–10), and therefore, it was unexpected to find situations where only one or the other cellular compartment was PD-L1 positive. To address this issue, we have retrospectively characterized a large cohort of NSCLC tumors and found that expression of PD-L1 by TC and IC was associated with different histological subtypes, with TC-positive tumors exhibiting a distinctive desmoplastic phenotype. In these tumors, invasive stromal elements were found adjacent to cancer cells that constitutively expressed the *PD-L1* gene due to hypomethylation of its promoter. Unlike the peritumoral stromal-rich histologies in other tumors (e.g., bladder cancer) that are associated with restricted T cell infiltration and poor response to atezolizumab (11), patients with desmoplastic NSCLC tumors respond favorably to therapy.

## Significance

**Programmed death-ligand 1 (PD-L1) expression on tumor cells and tumor-infiltrating immune cells is regulated by distinct mechanisms and has nonredundant roles in regulating anti-cancer immunity, and PD-L1 on both cell types is important for predicting best response to atezolizumab in non-small cell lung cancer.**

Author contributions: M. Kowanetz, S.N.G., P.S., J.C., N.A.R., D.R.S., A. Spira, D.S., Z.B., N.M., S.F., V.L., M.B., S.M., G.S., R.F., A. Sandler, I.M., D.S.C., and P.S.H. designed research; M. Kowanetz, W.Z., H.K., M. Kockx, and E.E.K. performed research; W.Z. contributed new reagents/analytic tools; M. Kowanetz, W.Z., S.N.G., P.S., I.W., F.R.H., V.C., D.S., G.H., L.A., I.M., D.S.C., and P.S.H. analyzed data; and M. Kowanetz, W.Z., S.N.G., H.K., M. Kockx, P.S., E.E.K., I.W., J.C., N.A.R., D.R.S., A. Spira, F.R.H., V.C., D.S., Z.B., N.M., S.F., V.L., D.S.S., M.B., S.M., G.S., R.F., G.H., A. Sandler, L.A., I.M., D.S.C., and P.S.H. wrote the paper.

Conflict of interest statement: M. Kowanetz, W.Z., H.K., E.E.K., D.S., Z.B., N.M., S.F., V.L., D.S.S., M.B., S.M., G.S., R.F., G.H., A. Sandler, L.A., I.M., D.S.C., and P.S.H. are full-time employees of Genentech, which supported the research described and markets the therapeutic antibody atezolizumab, under study.

This article is a PNAS Direct Submission.

This open access article is distributed under [Creative Commons Attribution-NonCommercial-NoDerivatives License 4.0 \(CC BY-NC-ND\)](https://creativecommons.org/licenses/by-nc-nd/4.0/).

<sup>1</sup>To whom correspondence may be addressed. Email: kowanetz.marcin@gene.com or mellman.ira@gene.com.

This article contains supporting information online at [www.pnas.org/lookup/suppl/doi:10.1073/pnas.1802166115/-DCSupplemental](http://www.pnas.org/lookup/suppl/doi:10.1073/pnas.1802166115/-DCSupplemental).

Published online October 8, 2018.

## Results

**Prevalence and Patterns of PD-L1 Expression in NSCLC.** Baseline tumor specimens from 4,549 first-line (1L) and 2L+ NSCLC patients received from four phase 1/2 atezolizumab trials (*SI Appendix, Fig. S1*) were analyzed for PD-L1 expression by trained pathologists [Food and Drug Administration (FDA)-approved complementary diagnostic SP142 immunohistochemistry (IHC) assay] (Fig. 1*A*). Differences among the various PD-L1 IHC reagents in NSCLC have been reported (12). Thus, to validate the results independently, we studied the association of PD-L1 expression on TC or IC at the validated diagnostic cutoffs with increasing *PD-L1* mRNA levels as an orthogonal measure of expression (Fig. 1*B*). The IHC analysis identified four distinct patterns of PD-L1 expression within the tumor microenvironment (TME): TC only, IC only, TC and IC, and neither TC nor IC expression (PD-L1 negative) (Fig. 1*C*). PD-L1 expression on IC was the predominant pattern. In the largest PD-L1-expressing subgroup (TC1/2/3 or IC1/2/3), ~33% of patients had tumors with PD-L1 expression restricted to IC, 6% had PD-L1 expression restricted to TC, and 26% had PD-L1 expression on both TC and IC (Fig. 1*C*). Notably, tumors displaying the highest levels of PD-L1 expression restricted to either TC (TC3) or IC (IC3) exhibited little overlap (~1% of the overall population) and thus, represent two distinct patient populations that have not been described before. We further confirmed the IC3-restricted expression of PD-L1 using a second FDA-approved PD-L1 IHC assay (SP263) in a nontrial cohort of NSCLC cases to independently confirm our findings (*SI Appendix, Fig. S2*). Given that the currently approved PD-L1 IHC companion diagnostics in NSCLC do not account for PD-L1 expression on IC, we aimed to study the biological factors associated with IC and TC expression of PD-L1 and the contribution of PD-L1 IC expression to outcomes for monotherapy treatment with atezolizumab.

**Molecular and Cellular Features Associated with PD-L1 Expression on TC and IC.** To study the molecular/cellular features associated with the differential expression of PD-L1 on TC vs. IC, we focused our analysis on PD-L1-negative (TC0 and IC0), TC3, and IC3 NSCLC tumor specimens as representative cases for the distinct patterns of PD-L1 expression observed. These tumors were comprehensively characterized by histopathology, gene expression, and methylation analyses. IC3 tumors were characterized by an immune-rich microenvironment (Fig. 2) with significantly higher numbers of cytotoxic CD8+ T cells within the tumor as well as higher numbers of overall tumor-infiltrating lymphocytes (TILs) (Fig. 2*A* and *B* and *SI Appendix, Fig. S3*). Furthermore, IC3 tumors were characterized by the contextual localization of immune infiltrates in the intraepithelial (Fig. 2*C*), epithelial-stromal interface (Fig. 2*D*), and stromal regions (Fig. 2*E* and *F*), whereas TC3 tumors were characterized by TILs largely confined to the peritumoral stromal region. Consistent with a highly infiltrated phenotype, IC3 tumors showed significantly higher expression of  $T_{eff}$ -associated genes (including *IFNG*, *GZMB*, and *CXCL9*) vs. TC3 tumors (Fig. 2*G* and *H* and *SI Appendix, Fig. S4*), suggesting IFN- $\gamma$ -mediated adaptive regulation of PD-L1 expression and the presence of a preexisting immune response in this subgroup of NSCLC tumors. Tumors with PD-L1 expression on both TC and IC displayed the TIL contexture and  $T_{eff}$  gene signature similar to those on IC3-restricted rather than TC3-restricted tumors, again reflecting an adaptive regulation of PD-L1 expression in this subgroup of tumors (Fig. 2*G* and *H* and *SI Appendix, Fig. S3*).

In contrast to IC3 tumors, TC3 tumors were characterized by a highly sclerotic (Fig. 3*A* and *C*) and desmoplastic (Fig. 3*B* and *C*) phenotype comprising extensive collagenized stroma, fibrous connective tissue, and activated fibroblasts that coursed throughout the tumor tissue (Fig. 3*C* and *SI Appendix, Fig. S5*). TC3 tumors also exhibited higher expression of markers associated with a mesenchymal phenotype and epithelial-mesenchymal transition

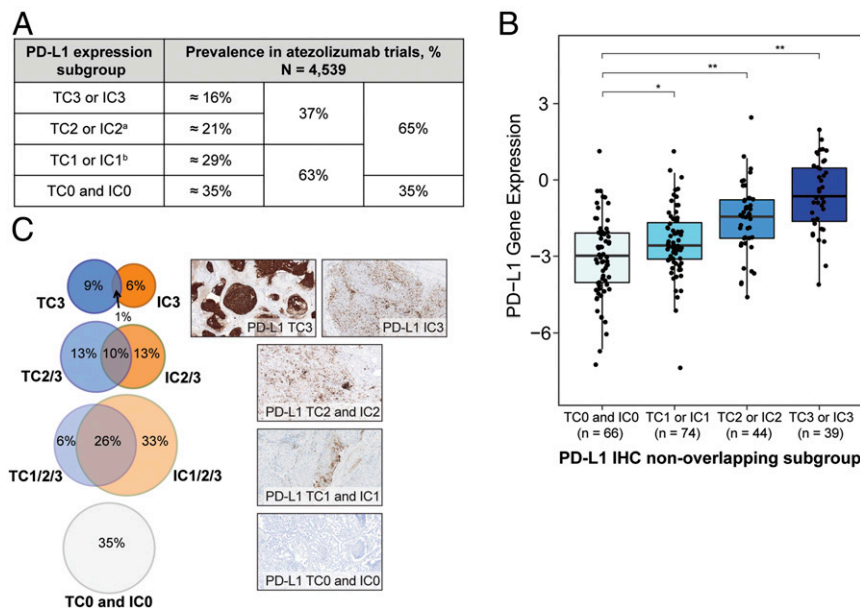


**Fig. 1.** Prevalence and patterns of PD-L1 expression on TC and IC. (*A*) Prevalence of PD-L1 in tumor biopsy specimens from patients prescreened and/or enrolled for the atezolizumab clinical trials FIR, BIRCH, and POPLAR. PD-L1 expression on TC and IC was determined by IHC and scored as described (*Materials and Methods*). <sup>a</sup>TC2/3 or IC2/3 excluding TC3 or IC3; <sup>b</sup>TC1/2/3 or IC1/2/3 excluding TC2/3 or IC2/3. (*B*) Association of PD-L1 protein expression with *PD-L1* mRNA in clinical specimens. Pretreatment tumor specimens from patients enrolled in the POPLAR trial binned into mutually exclusive subgroups based on PD-L1 IHC status on TC and IC. PD-L1 gene expression: \* $P < 0.05$  vs. TC0 and IC0 subgroups determined by Wilcoxon rank sum test; \*\* $P < 0.001$  vs. TC0 and IC0 subgroups determined by Wilcoxon rank sum test. (*C*) The Venn diagram (*Left*) illustrates the percentage overlap of PD-L1 on TC and IC relative to NSCLC tumor specimens from atezolizumab trials. Representative images (*Right*) of PD-L1 (brown) on TC and IC by IHC.



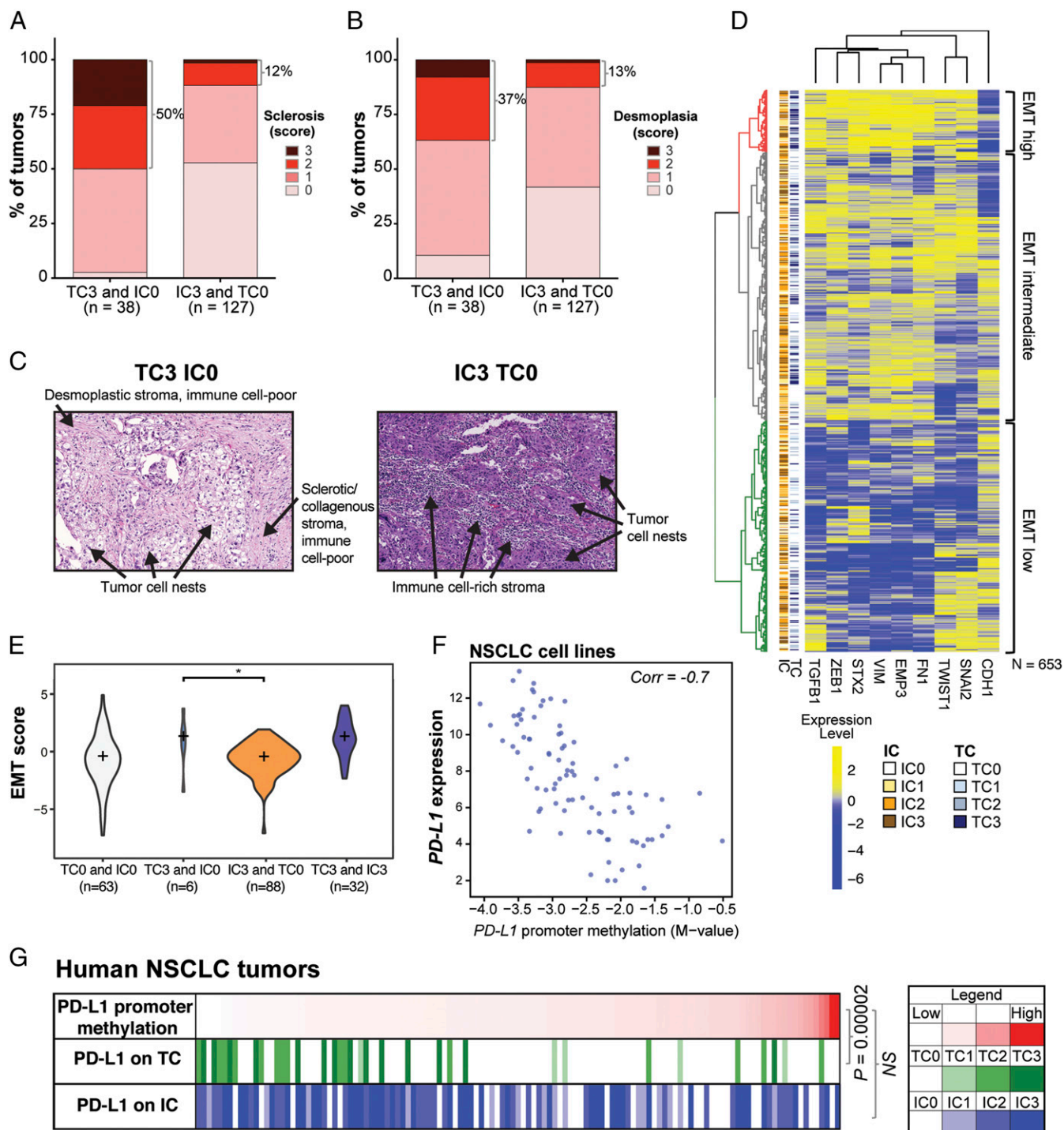


**Fig. 3.** TC3 tumors were characterized by a sclerotic/desmoplastic TME, mesenchymal markers expression, and epigenetic regulation of the *PD-L1* promoter. (A and B) TC3 and IC3 tumors scored for sclerosis and desmoplasia as described (*Materials and Methods*). (C) Representative images with H&E staining of TC3 and IC0 as well as IC3 and TC0 tumors. Sclerotic/desmoplastic characteristics of TC3 tumors are indicated with arrows. (D and E) High expression of EMT markers in TC3 tumors collected from lung. Plus signs in violin plot indicate median. *P* values were determined using the Wilcoxon rank sum test. (F and G) Correlation between *PD-L1* promoter methylation and PD-L1 expression in human NSCLC cell lines and tumors. *P* values are based on permutation tests in a multiple regression between log-transformed methylation and PD-L1 TC and IC scores.

First, we asked if the *PD-L1* gene may be amplified in a subset of NSCLC (17). Analysis of 276 tumors showed that 23% of TC3 tumors associated with increased *PD-L1* CN, indicating that gene amplification (defined as CN  $\geq 5$ ) can only partly account for high PD-L1 expression on TC (*SI Appendix, Fig. S8A*). Moreover, *PD-L1* CN gain was associated with the TC pattern of PD-

L1 but not the IC-restricted pattern of expression. Responses to atezolizumab were similarly observed in *PD-L1*-amplified vs. -nonamplified TC3 tumors (*SI Appendix, Fig. S8B*).

Second, we considered whether PD-L1 expression on TC is epigenetically regulated (18). Using human NSCLC cell lines ( $n = 150$ ), we found an inverse correlation between *PD-L1* gene

expression and the methylation of two noncanonical CpG sites (CpG1 and CpG5) near the STAT3 consensus binding regions within the *PD-L1* promoter (Fig. 3F). A similar phospho-STAT1 and phospho-STAT3 activation after IFN- $\gamma$  stimulation was observed in NSCLC cell lines with and without *PD-L1* promoter methylation, suggesting that the IFN- $\gamma$  signaling pathway was intact in TCs with the highly methylated *PD-L1* promoter (*SI Appendix*, Fig. S9). Consistent with the cell line data, in clinical samples, we also observed that increased PD-L1 expression on TC was most frequent in NSCLC tumors with reduced *PD-L1* promoter methylation (Fig. 3G). No association was found between PD-L1 IC and promoter methylation. Furthermore, analysis of peripheral blood mononuclear cells (PBMCs) revealed no methylation at CpG1 and rare methylation at CpG5 sites (*SI Appendix*, Fig. S10), confirming that TC expression, but not IC expression, is primarily associated with reduced *PD-L1* promoter methylation in NSCLC tumors.

Together, these data suggest that PD-L1 expression on TC3 may be regulated by tumor-intrinsic mechanisms involving gene CN gains and especially, promoter methylation.

**Efficacy of Atezolizumab in Patients with PD-L1 Expression on TC and IC.** We asked whether the different patterns of PD-L1 expression on TC and IC resulted in differential responses to atezolizumab in NSCLC. In a pooled analysis of 938 patients, high PD-L1 expression on TC or IC was independently associated with response to atezolizumab. Confirmed responses occurred in all categories of PD-L1 expression, including tumors with PD-L1 expression restricted to TC3 alone [objective response rate (ORR), 40%] or IC3 alone (ORR, 22%) (Fig. 4A and *SI Appendix*, Table S1). Response rates in patients with PD-L1-negative (TC0 and IC0) tumors were 8%. Patients in either TC3 alone or IC3 alone subgroups had similar durability of response (14.3 and 14.6 mo, respectively). Median progression-free survival (PFS) was 11.0 mo (95% CI, 1.6 to not estimable) for TC3-alone patients and 4.7 mo (95% CI, 2.8–5.8) for IC3-alone patients compared with 2.8 mo (95% CI, 1.5–4.2) for PD-L1-negative (TC0 and IC0) patients. Median OS was not reached (95% CI, 8.8 to not estimable) for TC3-alone patients and 17.9 mo (95% CI, 12.1 to not estimable) for IC3-alone patients compared with 10.0 mo (95% CI, 7.8–13.2) for PD-L1-negative patients (Fig. 4A and *SI Appendix*, Table S1). Thus, despite distinct regulation of PD-L1 expression, both TC3 and IC3 tumors responded favorably to atezolizumab, suggesting that both intrinsic and adaptive mechanisms regulating PD-L1 expression and expression on either TC or IC contribute to the antitumor immune response to atezolizumab in NSCLC.

We also investigated the time to response (TTR) and depth of response in tumors with distinct patterns of PD-L1 expression. Both TC3 and IC3 tumors exhibited comparable median TTR (2.74 mo for TC3 alone and 2.79 mo for IC3 alone), whereas numerically, the fastest median TTR (2 mo) seemed to be in patients expressing the highest levels of PD-L1 simultaneously on TC and IC (TC3 and IC3) (Fig. 4A and B). Depth of response was comparable across the subgroups (Fig. 4C). Notably, the few responding patients in the PD-L1-negative subgroup had a similar response pattern as in PD-L1-positive cases.

Despite the lower density of CD8+ T cells and TILs in TC3 tumors, especially in the intraepithelial region, the depth and duration of response (DOR) in these tumors suggested a T cell-dependent mechanism. We analyzed multiple baseline and on-treatment paired biopsies from a single TC3 responder to further investigate on-treatment modulation of T cell infiltration as a case report (Fig. 4D–F). While the baseline specimen exhibited poor intraepithelial CD8+ T cell infiltration with dense CD8+ T cell clusters restricted to the stroma, the on-treatment responding lesion collected ~6 mo after the first dose of atezolizumab (Fig. 4F) displayed a significant increase of CD8+ T cell

infiltration in the intraepithelial region (Fig. 4D), coincident with higher expression of T<sub>eff</sub> markers (*IFNG*, *GZMB*, and *PRF1*) and T cell chemoattractants (*CXCL9* and *CXCL10*) (Fig. 4E). Although limited by the number of such cases to gain mechanistic insights, this single case report provides preliminary evidence that ICs present in the surrounding stroma of TC3 responders may infiltrate the tumor and promote an antitumor immune response after inhibition of the PD-L1/PD-1 pathway.

## Discussion

Understanding the mechanism of action of PD-L1 and PD-1 is key to understanding the basis for or lack of response to immunotherapy and also for gaining confidence in the interpretation of results from PD-L1 IHC diagnostic assays, which are increasingly used for informing choice of treatment between checkpoint inhibitor (CPI) monotherapy and combination regimens in NSCLC (19–22). Clinical trials with PD-1 inhibitors have shown association between PD-L1 expression on TC and improved efficacy with anti-PD-1 agents compared with chemotherapy and led to FDA approval of pembrolizumab, with a companion diagnostic test for TC PD-L1 evaluation by IHC in NSCLC (4, 23). However, these studies did not assess PD-L1 expression on IC, which is now applied in the scoring algorithm for multiple PD-L1 tests across many indications, including metastatic urothelial carcinoma, head and neck cancer, and triple-negative breast cancer (24–27). The data described here show that tumors with PD-L1 expression on TC vs. IC differ on both the histological and the molecular levels. The characteristics of tumors with PD-L1 expression on IC and their association with patient outcomes with atezolizumab monotherapy are consistent with our previous observations that the T<sub>eff</sub> gene signature is associated with improved efficacy for atezolizumab vs. docetaxel in the POPLAR and OAK studies (7, 28) and consistent with similar observations reported with other PD-L1 or PD-1 inhibitors in multiple tumor types (29–31). In addition, these data further strengthen the concept that ICs can act not only to restrict T cell activity (by presenting a source of PD-L1) but also, to facilitate an initial intratumoral expansion of T cells by providing CD80 and CD86 for CD28-dependent T cell costimulation; PD-1 on T cells acts at least in part by regulating CD28 signaling (32, 33). Nonredundant roles for PD-L1 expression on IC and TC are also consistent with recent observations in mice, where genetic manipulation was used to show contributions for tumor vs. host-derived PD-L1 in controlling antitumor immunity (34, 35).

It is thus increasingly clear that ICs play a critical role in regulating T cell responses independent of PD-L1 expression by TC. Our clinical and nonclinical studies point to a role of IC expression of PD-L1 as an important indicator of preexisting immunity and active immune suppression in the tumor milieu. Blockade of PD-L1/PD-1 signaling axis by CPIs overcomes this suppression. Therefore, PD-L1 expression on IC is a relevant biomarker to identify patients with tumors that are poised to respond to checkpoint inhibition and is consistent with many previous studies (both clinical and preclinical) that have shown PD-L1 expression in tumors as an “adaptive response” to IFN- $\gamma$  release by T<sub>eff</sub> cells.

We also observed a subset of NSCLC tumors where TCs exhibit the cell-autonomous and T cell-independent expression of PD-L1 apparently due to such mechanisms as promoter demethylation or gene amplification. Despite the absence of demonstrable PD-L1-positive ICs, these tumors also respond well to atezolizumab, strongly suggesting preexisting immunity, although there was little T cell infiltration detected. Presumably, epigenetically dysregulated TC clones endogenously expressing PD-L1 were selected for survival and growth due to their ability to create a strong immunosuppressive environment and attenuate T cell-mediated rejection. These tumors also exhibited a distinctive desmoplastic phenotype characterized by



## Materials and Methods

**Tumor Specimens.** Baseline archival or freshly collected resections and biopsies were obtained from 1L and 2L+ patients with metastatic NSCLC who were prescreened and/or enrolled in the atezolizumab trials PCD4989g, FIR, POPLAR, and BIRCH. These trials were sponsored by Genentech, Inc., a member of the Roche Group, which provided the study drug, atezolizumab. The protocols and their amendments were approved by the relevant institutional review boards or ethics committees, and all participants provided written informed consent. The clinical trials from which the data were derived were conducted in accordance with the Declaration of Helsinki and International Conference on Harmonization Guidelines for Good Clinical Practice: ClinicalTrials.gov: NCT01375842 (<https://clinicaltrials.gov/ct2/show/NCT01375842>), NCT01846416 (<https://clinicaltrials.gov/ct2/show/NCT01846416>), NCT01903993 (<https://clinicaltrials.gov/ct2/show/NCT01903993>), and NCT02031458 (<https://clinicaltrials.gov/ct2/show/NCT02031458>). In addition, tumor specimens from a cohort of nontrial patients with advanced NSCLC who were not treated with anti-PD-L1/PD-1 agents were included in this analysis.

**Treatment Outcomes Groups.** Efficacy was assessed according to Response Evaluation Criteria in Solid Tumors (RECIST) v1.1 (39). PCD4989g (NCT01375842) is a multicenter, open label, dose escalation and expansion, phase 1 study of atezolizumab administered to patients with locally advanced or metastatic solid tumors or hematologic malignancies (40). Patients were either enrolled regardless of PD-L1 status or selected based on PD-L1 expression depending on the study cohort. Briefly, patients received atezolizumab at doses up to 20 mg/kg i.v. every 3 wk. Radiological assessments were performed every 6 wk for 24 wk and every 12 wk thereafter per RECIST v1.1. Patients who were evaluable for efficacy (per RECIST v1.1) had measurable disease at baseline and received atezolizumab  $\geq 1$  mg/kg. The clinical data cutoff was December 2, 2014.

FIR (NCT01846416) is a multicenter, single-arm, phase 2 study of atezolizumab in patients with PD-L1–selected locally advanced or metastatic NSCLC. Patients received atezolizumab 1,200 mg i.v. every 3 wk. Tumor responses were evaluated at baseline and every 6 wk thereafter for the first 12 mo after cycle 1, day 1; after 12 wk, tumor assessments occurred every 9 wk. The clinical data cutoff was January 7, 2015.

POPLAR (NCT01903993) is a multicenter, open label, randomized, phase 2 study of atezolizumab compared with docetaxel in patients with NSCLC after platinum chemotherapy failure. Patients were stratified as previously described (7) and randomized to receive atezolizumab 1,200 mg i.v. every 3 wk or docetaxel 75 mg/m<sup>2</sup> i.v. every 3 wk. Tumors were assessed at baseline, 6 wk, every 6 wk thereafter for 36 wk after randomization, and every 9 wk thereafter. The primary analysis was based on 173 events, with a minimum follow-up of 13 mo at the clinical data cutoff of May 8, 2015.

BIRCH (NCT02031458) is a multicenter, single-arm, phase 2 study of atezolizumab in patients with PD-L1–selected locally advanced or metastatic NSCLC. Patients received atezolizumab 1,200 mg i.v. every 3 wk until loss of clinical benefit as assessed by the investigator. Tumor responses were evaluated at baseline and every 6 wk thereafter for the first 12 mo after cycle 1, day 1, and then, they were evaluated every 9 wk thereafter. The clinical data cutoff was May 28, 2015.

**IHC Analysis for PD-L1, CD8, and PD-1.** Formalin-fixed, paraffin-embedded (FFPE) tumor tissue from biopsies and resections collected before atezolizumab treatment was used for PD-L1 and CD8 analysis by IHC. PD-L1 expression was assessed with the VENTANA SP142 assay, which is sensitive and specific for PD-L1 expression on both TC and IC (40). PCD4989g specimens were scored using the prototype assay; FIR, POPLAR, and BIRCH specimens were scored using an investigational use only assay. PD-L1 expression was scored at four levels based on increasing expression as described (7). PD-L1 TC expression was scored as the percentage of TC stained positive as follows: TC3:  $\geq 50\%$  of TC PD-L1; TC2:  $\geq 5\%$  but  $< 50\%$  of TC PD-L1; TC1:  $\geq 1\%$  but  $< 5\%$  of TC PD-L1; and TC0:  $< 1\%$  of TC PD-L1. PD-L1 IC expression was scored as the percentage of tumor area stained positive as follows: IC3:  $\geq 10\%$  PD-L1; IC2:  $\geq 5\%$  but  $< 10\%$  PD-L1; IC1:  $\geq 1\%$  but  $< 5\%$  PD-L1; and IC0:  $< 1\%$  PD-L1. A subset of nontrial NSCLC specimens was also stained for PD-L1 with the VENTANA SP263 assay and scored for PD-L1 expression on TC. CD8 expression (clone C8/144B) was assessed in the tumor center, invasive margin, and periphery in available specimens from PCD4989g and FIR studies. PD-1 expression was assessed on TC and IC in a cohort of nontrial specimens using clone NAT105 and scored as the percentage of cells expressing PD-1. In all specimens, total immune infiltrate was assessed in the tumor area based on H&E staining.

**Histopathologic Analysis.** Histopathologic assessment of the available TC3 (IC0/1) and/or IC3 (TC0) tumor specimens from the FIR, POPLAR, and BIRCH studies ( $n = 204$ ) included the presence of IC at the interface between tumor and stroma, intraepithelial IC, IC in the tumor stroma, fibrous connective tissue with persistence of activated fibroblasts (desmoplasia), or cell-poor/collagenized stroma (sclerotic stroma). An estimated score of zero to three was assigned to each category as follows.

Interface activity was defined as the presence of ICs at the border of the tumor strands and in the immediately adjacent stroma. The interface activity in the tumor area was scored as follows: zero, 0% activity; one, focal interface activity; two, more than focal interface activity but  $< 50\%$  of tumor strands showing regions of interface activity; or three,  $\geq 50\%$  of tumor strands showing regions of interface activity.

Intraepithelial/intratatumoral ICs were identified as those located within the tumor strands. Intratumoral epithelial ICs were defined as ICs in tumor nests having no cell-to-cell contact with intervening stroma and directly interacting with carcinoma cells. The presence of this feature in the tumor area was scored as follows: zero, 0% intraepithelial/intratatumoral ICs; one, focal intraepithelial/intratatumoral ICs; two, more than focal intraepithelial/intratatumoral ICs but  $< 50\%$  of tumor strands showing intraepithelial/intratatumoral ICs; or three,  $\geq 50\%$  of tumor strands showing intraepithelial/intratatumoral ICs.

Stromal ICs were scored uniquely as a percentage of the stromal areas alone. The areas occupied by carcinoma cells were not included in the total assessed surface area.

Sclerotic stroma was defined as cell-poor, collagenous fiber-rich stroma and assigned a score of zero (absence of sclerosis) to three (strong sclerotic reaction). Desmoplastic stroma was defined as fibrous connective tissue with the presence of activated fibroblasts and assigned a score of zero (absence of desmoplasia) to three (strong desmoplastic reaction).

**DNA and RNA Isolation from FFPE Tumor Tissue.** DNA and RNA isolation was performed as described previously (41). Briefly, tumor tissue from FFPE sections was lysed using tumor lysis buffer and proteinase K to allow for complete digestion and release of nucleic acids. Specimens were macrodissected if tumor content was  $< 70\%$  to enrich for neoplastic tissue before the lysis. RNA was isolated using the High Pure FFPE RNA Micro Kit (Roche Diagnostics) according to the manufacturer's protocol. DNA was isolated using the QIAamp DNA FFPE Tissue Kit (Qiagen) according to the manufacturer's protocol. RNA and DNA were stored at  $-80^\circ\text{C}$  until the analyses were performed.

**Gene Expression Analysis.** iChip or RNAseq (Expression Analysis, Inc.) was used to assess gene expression in tumors with available RNA from PCD4989g ( $n = 73$  for iChip and  $n = 53$  for RNAseq), FIR ( $n = 127$  for iChip and  $n = 95$  for RNAseq), POPLAR ( $n = 225$  for iChip and  $n = 193$  for RNAseq), BIRCH ( $n = 618$  for iChip and  $n = 591$  for RNAseq), and the nontrial cohort ( $n = 78$  for RNAseq). RNAseq data were normalized via voom (42) using size factors estimated by DESeq2 (43) within individual trials and were log<sub>2</sub> transformed for nontrial samples. All RNAseq data were renormalized against sample medians before pooling. For gene signature analysis, expression values were standardized within individual genes and averaged across relevant genes. The T<sub>eff</sub> gene signature was defined by expression of *CD8A*, *GZMA*, *GZMB*, *IFNG*, *EOMES*, *CXCL9*, *CXCL10*, and *TBX21*. The EMT gene signature was defined by expression of *TGFB1*, *ZEB1*, *STX2*, *VIM*, *EMP3*, *FN1*,  *Twist1*, *SNAI2*, and *CDH1*. To exclude a possibility that the observed differences in T<sub>eff</sub> and EMT gene expression were due to differences in TC content between the TC3 and IC3 subsets, tumor specimens were also analyzed for *TFE1* and *p63* gene expression.

**Gene CN Analysis.** The FoundationOne panel (Foundation Medicine) was used to analyze PD-L1 gene amplification. An increase in CN was defined as five or more copies.

**Epigenetic Analysis.** PD-L1 promoter methylation in 88 NSCLC cell lines [ATCC ( $n = 67$ ), JHSF ( $n = 7$ ), DMSZ ( $n = 5$ ), UTSW ( $n = 5$ ), NCI-DCTD ( $n = 30$ ), NCI-GEO ( $n = 1$ )] and 150 NSCLC nontrial tumor samples was assessed by sodium bisulfite next generation sequencing. All cell lines were authenticated by internal short tandem repeat analysis and were verified to be mycoplasma free using the MycoAlert (Lonza) and/or MycoSensor (Agilent) assay kit (44). Tumor specimens were enriched for tumor content by macrodissection before DNA isolation. Directed hierarchical clustering was used to analyze the results. For assessment of the contribution of TC vs. IC in PD-L1 promoter methylation in TC, IC, and other cell types, clonal bisulfite sequencing was performed. Briefly, DNA was amplified from transformed normal lung cell lines (gBEC1 and gSAC1) (13), NSCLC cell lines (A427, H2073, and H358), and pooled PBMCs by custom PCR primers flanking the CpG region in the PD-L1 promoter represented on the

Infinium HumanMethylation450 array (Illumina). DNA from selected clones was extracted and prepared for standard bisulfite sequencing.

**Statistical Analysis.** Clinical outcome end points were summarized for patients who received atezolizumab. Investigator-assessed ORRs, confirmed per RECIST v1.1, were based on the proportion of patients who had a best response of complete response or partial response. OS was the time between the date of randomization or first atezolizumab dose and death due to any cause. PFS was the time between the date of randomization/first atezolizumab dose and the date of first documented disease progression or death, whichever occurred first; disease progression was determined based on investigator assessment per RECIST v1.1. DOR was the time from the first occurrence of a documented

objective response to the time of disease progression as determined by investigator per RECIST v1.1 or death from any cause, whichever occurred first. The 95% CIs were exact CIs for ORRs and plain CIs for OS, PFS, and DOR.

**ACKNOWLEDGMENTS.** We thank the patients and their families as well as all of the investigators and their staff involved in PCD4989g, FIR, BIRCH, and POPLAR. From Genentech, we thank C. Ahearn, J. Yi, P. He, Z. Li, B. Lyons, G. Fine, M. Denker, C. Cummings, N. Patil, and K. Walter (currently at Corvus Pharmaceuticals). Support for third-party writing assistance for this manuscript was provided by Meghal Gandhi and Jessica Bessler (Health Interactions) and funded by F. Hoffmann-La Roche Ltd. This study was funded by Genentech, Inc. and F. Hoffmann-La Roche Ltd.

- Genentech, Inc. (2017) Tecentriq (atezolizumab) package insert (Genentech, Inc., South San Francisco, CA).
- Merck & Co, Inc. (2017) Keytruda (pembrolizumab) package insert (Merck & Co, Inc., Whitehouse Station, NJ).
- Bristol-Myers Squibb (2017) Opdivo (nivolumab) package insert (Bristol-Myers Squibb, New York).
- Borghaei H, et al. (2015) Nivolumab versus docetaxel in advanced nonsquamous non-small-cell lung cancer. *N Engl J Med* 373:1627–1639.
- Reck M, et al.; KEYNOTE-024 Investigators (2016) Pembrolizumab versus chemotherapy for PD-L1-positive non-small-cell lung cancer. *N Engl J Med* 375:1823–1833.
- Rittmeyer A, et al.; OAK Study Group (2017) Atezolizumab versus docetaxel in patients with previously treated non-small-cell lung cancer (OAK): A phase 3, open-label, multicentre randomised controlled trial. *Lancet* 389:255–265.
- Fehrenbacher L, et al.; POPLAR Study Group (2016) Atezolizumab versus docetaxel for patients with previously treated non-small-cell lung cancer (POPLAR): A multicentre, open-label, phase 2 randomised controlled trial. *Lancet* 387:1837–1846.
- Yamazaki T, et al. (2002) Expression of programmed death 1 ligands by murine T cells and APC. *J Immunol* 169:5538–5545.
- Brown JA, et al. (2003) Blockade of programmed death-1 ligands on dendritic cells enhances T cell activation and cytokine production. *J Immunol* 170:1257–1266.
- Loke P, Allison JP (2003) PD-L1 and PD-L2 are differentially regulated by Th1 and Th2 cells. *Proc Natl Acad Sci USA* 100:5336–5341.
- Mariathasan S, et al. (2018) TGF $\beta$  attenuates tumour response to PD-L1 blockade by contributing to exclusion of T cells. *Nature* 554:544–548.
- Hirsch FR, et al. (2017) PD-L1 immunohistochemistry assays for lung cancer: Results from phase 1 of the blueprint PD-L1 IHC assay comparison project. *J Thorac Oncol* 12:208–222.
- Walter K, et al. (2012) DNA methylation profiling defines clinically relevant biological subsets of non-small cell lung cancer. *Clin Cancer Res* 18:2360–2373.
- Chen L, et al. (2014) Metastasis is regulated via microRNA-200/ZEB1 axis control of tumour cell PD-L1 expression and intratumoral immunosuppression. *Nat Commun* 5:5241.
- Travis WD, et al.; American Thoracic Society (2011) International Association for the Study of Lung Cancer/American Thoracic Society/European Respiratory Society: International multidisciplinary classification of lung adenocarcinoma: Executive summary. *Proc Am Thorac Soc* 8:381–385.
- Shames DS, Wistuba II (2014) The evolving genomic classification of lung cancer. *J Pathol* 232:121–133.
- Rooney MS, Shukla SA, Wu CJ, Getz G, Hacohen N (2015) Molecular and genetic properties of tumors associated with local immune cytolytic activity. *Cell* 160:48–61.
- Wrangle J, et al. (2013) Alterations of immune response of non-small cell lung cancer with azacytidine. *Oncotarget* 4:2067–2079.
- Chen DS, Mellman I (2013) Oncology meets immunology: The cancer-immunity cycle. *Immunity* 39:1–10.
- Kim JM, Chen DS (2016) Immune escape to PD-L1/PD-1 blockade: Seven steps to success (or failure). *Ann Oncol* 27:1492–1504.
- Festino L, et al. (2016) Cancer treatment with anti-PD-1/PD-L1 agents: Is PD-L1 expression a biomarker for patient selection? *Drugs* 76:925–945.
- Zou W, Wolchok JD, Chen L (2016) PD-L1 (B7-H1) and PD-1 pathway blockade for cancer therapy: Mechanisms, response biomarkers, and combinations. *Sci Transl Med* 8:328rv4.
- Topalian SL, et al. (2012) Safety, activity, and immune correlates of anti-PD-1 antibody in cancer. *N Engl J Med* 366:2443–2454.
- Rosenberg JE, et al. (2016) Atezolizumab in patients with locally advanced and metastatic urothelial carcinoma who have progressed following treatment with platinum-based chemotherapy: A single-arm, multicentre, phase 2 trial. *Lancet* 387:1909–1920.
- Plimack ER, et al. (2017) Safety and activity of pembrolizumab in patients with locally advanced or metastatic urothelial cancer (KEYNOTE-012): A non-randomised, open-label, phase 1b study. *Lancet Oncol* 18:212–220.
- Seiwert TY, et al. (2016) Safety and clinical activity of pembrolizumab for treatment of recurrent or metastatic squamous cell carcinoma of the head and neck (KEYNOTE-012): An open-label, multicentre, phase 1b trial. *Lancet Oncol* 17:956–965.
- Schmid P, et al. (2017) Abstract 2986: Atezolizumab in metastatic triple-negative breast cancer: Long-term clinical outcomes and biomarker analyses. *Cancer Research* 77(Suppl 13):2986–2986.
- Kowanetz M, et al. (2017) Pre-existing immunity measured by teff gene expression in tumor tissue is associated with atezolizumab efficacy in NSCLC. *J Thorac Oncol* 12(Suppl 2):S1817–S1818.
- Higgs B, et al. (2015) High tumoral IFN $\gamma$  mRNA, PD-L1 protein, and combined IFN $\gamma$  mRNA/PD-L1 protein expression associates with response to durvalumab (anti-PD-L1) monotherapy in NSCLC patients. *Eur J Cancer* 51(Suppl 3):S717.
- Muro K, et al. (2015) Relationship between PD-L1 expression and clinical outcomes in patients (pts) with advanced gastric cancer treated with the anti-PD-1 monoclonal antibody pembrolizumab (pembro; MK-3475) in KEYNOTE-012. *J Clin Oncol* 33(Suppl 3):3.
- Seiwert TY, et al. (2015) Antitumor activity and safety of pembrolizumab in patients (pts) with advanced squamous cell carcinoma of the head and neck (SCCHN): Preliminary results from KEYNOTE-012 expansion cohort. *J Clin Oncol* 33(Suppl 18):LBA6008.
- Hui E, et al. (2017) T cell costimulatory receptor CD28 is a primary target for PD-1-mediated inhibition. *Science* 355:1428–1433.
- Kamphorst AO, et al. (2017) Rescue of exhausted CD8 T cells by PD-1-targeted therapies is CD28-dependent. *Science* 355:1423–1427.
- Lau J, et al. (2017) Tumour and host cell PD-L1 is required to mediate suppression of anti-tumour immunity in mice. *Nat Commun* 8:14572.
- Juneja VR, et al. (2017) PD-L1 on tumor cells is sufficient for immune evasion in immunogenic tumors and inhibits CD8 T cell cytotoxicity. *J Exp Med* 214:895–904.
- Eroglu Z, et al. (2018) High response rate to PD-1 blockade in desmoplastic melanomas. *Nature* 553:347–350.
- Hegde PS, Karanikas V, Evers S (2016) The where, the when, and the how of immune monitoring for cancer immunotherapies in the era of checkpoint inhibition. *Clin Cancer Res* 22:1865–1874.
- Chen DS, Mellman I (2017) Elements of cancer immunity and the cancer-immune set point. *Nature* 541:321–330.
- Eisenhauer EA, et al. (2009) New response evaluation criteria in solid tumours: Revised RECIST guideline (version 1.1). *Eur J Cancer* 45:228–247.
- Herbst RS, et al. (2014) Predictive correlates of response to the anti-PD-L1 antibody MPDL3280A in cancer patients. *Nature* 515:563–567.
- Schleifman EB, et al. (2014) Targeted biomarker profiling of matched primary and metastatic estrogen receptor positive breast cancers. *PLoS One* 9:e88401.
- Law CW, Chen Y, Shi W, Smyth GK (2014) Voom: Precision weights unlock linear model analysis tools for RNA-seq read counts. *Genome Biol* 15:R29.
- Love MI, Huber W, Anders S (2014) Moderated estimation of fold change and dispersion for RNA-seq data with DESeq2. *Genome Biol* 15:550.
- Yu M, et al. (2015) A resource for cell line authentication, annotation and quality control. *Nature* 520:307–311.